Indian J. Phys. **76B** (4), 379–385 (2002)

I J P B
— an international journal

Single and multiple ionization of atoms by electron impact

Hubert Klar

Theoretical Quaantumdynamics, Albert-Ludwige-Universität, Herman Herder Strasse 3, 79104 Freiburg, Germany
E-mail : klarhub@RUF UNI-FREIBURG DE

Abstract : We report progress achieved during decades on direct single and multiple ionization of simple atoms by electron collsion. In particular we investigate total cross sections from threshold to high energies. We show that all experimental data compare favorably with Wannier threshold theory. A better understanding of the ionization process one gets from the analysis of multiply differential cross sections. To this end we discuss $(e, 2e)$ and $(e, 3e)$ events.

Keywords : Single, multiple, ionisation, electron, atom

PACS No. . 34.80.Dp

1. Introduction

The electron impact ionization of atoms has been known now for nearly 100 years. Quantitative measurements, however, mostly for total cross sections have been performed during 1920 through 1970, using parallel plate configurations for the collection of the produced ions [1] or using mass spectrometry [2]. Particularly during the last 30 years detailed experimental and theoretical research has been carried out although for many targets only little or no data exist. The reasons for that lack are based on the experimental difficulties of the preparation of the targets and of selective detection of the different types of ionization processes. From the theoretical viewpoint the description of an ionization event needs at least a 3-body scattering theory valid for long range Coulomb interactions. But such a theory is not available. Therefore early calculations were based on a first order perturbation treatment, also known as Born approximation or Bethe theory [3]. Below we will summarize Bethes development including applications because many present calculations are still based on that theory. It is not the purpose to summarize all previous work on atomic ionization, only key work including latest results will be mentioned. This recent work also involves coincidence measurements, *i.e.* $(e, 2e)$ and $(e, 3e)$ processes. Atomic units are used throughout this paper.

2. Total cross sections

Total cross sections are known for a variety of gas targets. Measurements for H, *i.e.* the reaction

$$e + \mathrm{H}\,(1s) \rightarrow \mathrm{H}^{+} + e + e \qquad (1)$$

have been performed by several authors, see for instance [4] for an overview. Figure 1 shows H data. It is evident that the cross section has one single maximum.

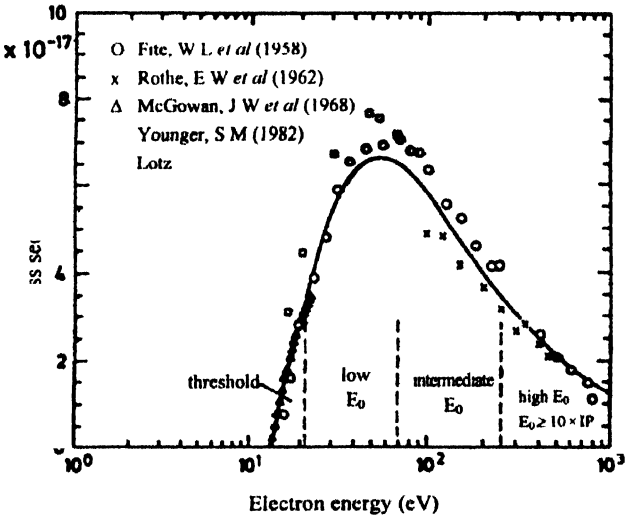

Figure 1. Total cross section for electron impact ionization of H(1*s*) as a function of impact energy.

The cross section tends to zero both at high energies as well as at threshold. The behavior at high incident energy can be evaluated analytically on the basis of the first Born approximation [3,5]. The Born approximation applies here because high-energy collisions are usually accompanied with small momentum transfer. It can than be shown that the total cross section at constant energy transfer decreases as given by

$$\lim_{E\to\infty} \sigma \propto \frac{\log E}{E} \tag{2}$$

Therefore, one conveniently plots $E\sigma$ *versus* $\log E$. This plot, socalled Fano-Plot, shows at high energies a straight line whose slope determines the optical oscillatorstrenth, see for instance [5].

At threshold the situation is more difficult. From phase space considerations one would expect a linear threshold law. Correlation is expected however to modify this simple fact. Over the years many threshold laws have been published, most of them however are wrong because of unrealistic assumptions on the correlation. Only Wannier [9] seems to have solved that problem. His threshold law reads

$$\lim_{E\to 0} \sigma_{\text{total}} \propto (E-E_0)^{\mu-\frac{1}{4}} \tag{3}$$

with E_0 being the threshold energy and μ being a characteristic exponent given by

$$\frac{1}{4}\sqrt{\frac{100Z-9}{4Z-1}} \tag{4}$$

where Z is the charge of the formed ion. So, for instance, ionization of a neutral atom leads to $Z = 1$ and therefore, to $\mu - \frac{1}{4} = 1.127....$ This theory is based on the following ingredients :

- Classical mechanics does apply.
- Double escape near threshold occurs through trajectories along an unstable potential ridge.
- The instability results from competive ineleastic scattering leading to single escape.
- The motion within the reaction zone is irregular .
- The cross section is identified as time derivative of the phase space volume at constant energy.

These ingredients lead to the following general properties of the Wannier law :

- The threshold law is valid for any ionization mechanism, for instance electron impact ionization, photo double ionization.
- The energy distribution of the escaping electrons is flat, *i.e.* any energy sharing is equally likely.
- The electrons escape into opposite directions.

For a long time the Wannier law was simply not believed in the community. But in the meantime we have an overwhelming experimental material confirming Wanniers threshold law. This data is summarized in Table 1.

Table 1. Summary of experimental and theoretical date of threshold ionization processes, see text.

Target	Projectile	Ion	n (exp)	n (theor)	Reference
He	e	He(1s)	1.131 ± 0.019	1.127	[7]
He	γ	He^{++}	1.06	1.06	[8]
Ne	e	$Ne(K^{-1})^{+}$	1.13 ± 0.04	1.127	[9]
Ar	e	$Ar(K^{-1})^{+}$	1.10 ± 0.04	1.127	[10]
H^-	γ	H^{+}	1.15 ± 0.04	1.127	[11]
N	γ	N^{+++}	2.17	2.162	[12]
O	γ	O^{+++}	2.176	2.162	[12]

Inspection of Table 1 shows favorable agreement between experimental data and Wanniers prediction. In the case of innershell ionization the experimental data shows a remarkably large energy range of validity [9]. Qualitatively this is understandable because roughly the ratio of excess energy over the binding energy enters into the wavefunction not the absolute value of the excess senergy [13]. The Wannier theory has been extended to more than 2 escaping electrons [14]. For triple escape in a singlett spin state Klar and Schlecht [14] have predicted the characteristique exponent $n = 2.162$ which compares favorably with Samsons measurements [12].

3. Scattering theory

We treat here the theoretical frame to calculate triply differential cross sections (TDCS) for $(e, 2e)$-reactions. The TDCS for two escaping electrons (scattered and ionized electron, respectively) is formally given by

$$\frac{d^3\sigma}{d\Omega_a d\Omega_b dE_b} = (2\pi)^4 \frac{k_a k_b}{k_0} |T_{if}| \tag{5}$$

where $\boldsymbol{k}_0$, $\boldsymbol{k}_a$, $\boldsymbol{k}_b$ are the momenta of the incident, scattered and ejected electron, respectively. The T-matrix element is given by

$$T_{if} = \langle \Psi_f^- | V | \Phi \rangle \tag{6}$$

Here the initial state Φ is a product state consisting of a plane wave for the incoming electron and a bound state wave function for the target atom. V is the (non-relativistic) potential between the projectile and the target, and Ψ_f^- is the final state describing two escaping electrons in the field of an ion; *i.e.* this should be an exact solution of the $N+1$ electron problem.

An exact solution Ψ_f^- of course is not available. The following approximations have been frequently used in the literature.

3.1 Plane wave approximation :

This simple approximation disregards any interaction and treats both electrons as free particles, *i.e.*

$$\Psi_f^- = (2\pi)^{-3} e^{i(\boldsymbol{k}_a \cdot \boldsymbol{r}_a + \boldsymbol{k}_b \cdot \boldsymbol{r}_b)} \tag{7}$$

3.2 Born approximation :

This approximation, also known as Bethe [3] approximation, is applicable at low values of the momentum transfer, *i.e.* at relatively fast incident electrons, fast scattered and much slower secondary electrons. This approximation treats the fast scattered electron again as a plane wave (free particle) and the secondary electron is represented by an ordinary Coulomb wave $\psi_{k_b}(\boldsymbol{r}_b)$,

$$\Psi_f^-(2\pi)^{-3/2} e^{i\boldsymbol{k}_a \cdot \boldsymbol{r}_a} \psi_{k_b}(\boldsymbol{r}_b) \tag{8}$$

This implies that the interaction of the slower electron with the ion (often a bare nucleus) is taken into account, but all other interactions in the final state are disregarded. Nice and useful applications of the Born approximation are discussed in §4.1 and §4.2.

3.3 BBK :

A further improvement of the wavefunction is provided by taking into account both electron-ion interactions as well as the electron-electron repulsion. Exactly this is done by a wavefunction, see also [15,16], of the following form

$$\begin{aligned}\Psi_f^- = (2\pi)^{-3/2} & e^{i(\boldsymbol{k}_a \cdot \boldsymbol{r}_a + \boldsymbol{k}_b \cdot \boldsymbol{r}_b)} \\ & \times {}_1F_1\left(-i\frac{Z}{k_a}, 1; -i(k_a r_a + \boldsymbol{k}_a \cdot \boldsymbol{r}_a)\right) \\ & \times {}_1F_1\left(-i\frac{Z}{k_b}, 1; -i(k_b r_b + \boldsymbol{k}_b \cdot \boldsymbol{r}_b)\right) \\ & \times {}_1F_1\left(i\frac{1}{2\kappa}, 1; -i(\kappa r_{ab} + \boldsymbol{\kappa} \cdot \boldsymbol{r}_{ab})\right)\end{aligned} \tag{9}$$

with $\boldsymbol{\kappa} = \frac{1}{2}(\boldsymbol{k}_a - \boldsymbol{k}_b)$ and $\boldsymbol{r}_{ab} = \boldsymbol{r}_a - \boldsymbol{r}_b$. The essential property of this wavefunction is that it shows exact asymptotic behaviour in the Redmond [17] limit, *i.e.* for large particle separations.

3.4 Local momenta :

An even better description of the double continuum state is achieved with help of local space dependent momenta [18], see also [19]. Actually Alt and Mukhamedzhanov [18] showed the nessecity of modified momenta to correctly describe the asymptotic form of the wavefunction in the limiting case of one particle far away from the remaining 2-body subsystem. We present here a slightly different view point and proceed as follows. First we separate off the plane wave factor for the electrons

$$\Psi_f^- = e^{i(\boldsymbol{k}_> \cdot \boldsymbol{r}_> + \boldsymbol{k}_< \cdot \boldsymbol{r}_<)} \overline{\Psi} \tag{10}$$

where $\overline{\Psi}$ describes the Coulomb modifications. $r_{>,(<)}$ stands for the larger (smaller) electron-ion separation, and $k_{>,(<)}$ are the corresponding momenta. As in the BBK wave-function, eq. (9), we employ Coulomb waves for 2-body subsystems. For the outer electron located at $r_>$ we use ordinary Coulomb waves for the 2-body subsystem as above,

$$\begin{aligned}\overline{\Psi} = A\, {}_1F_1\left(-i\frac{Z}{k_>}, 1; -i(k_> r_> + \boldsymbol{k}_> \cdot \boldsymbol{r}_>)\right) \times \\ {}_1F_1\left(i\frac{1}{2\kappa}, 1; -i(\kappa r + \boldsymbol{\kappa} \cdot \boldsymbol{r})\right) \propto A e^{i\Phi}\end{aligned} \tag{11}$$

where the phase Φ being chosen to produce correct asymptotic behaviour,

$$\left(\boldsymbol{k}_> \cdot \vec{\nabla}_> + \boldsymbol{k}_< \cdot \vec{\nabla}_<\right)\Phi = \frac{Z}{r_>} + \frac{1}{r_{><}} \tag{12}$$

with the solution

$$\Phi = \frac{Z}{k_>} \ln\left(k_> r_> + \boldsymbol{k}_> \cdot \boldsymbol{r}_> - \frac{1}{2\kappa} \ln(\kappa r_{><} + \boldsymbol{\kappa}(\boldsymbol{r}_> - \boldsymbol{r}_<)\right) \tag{13}$$

and $\boldsymbol{\kappa} = \frac{1}{2}(\boldsymbol{k}_> - \boldsymbol{k}_<)$. The amplitude in eq. (11) describes the motion of the inner electron located at $r_<$. For $r_> \gg r_<$ the wave equation for $A = A(r_<)$ redues to

$$\left[\nabla_< + 2i\boldsymbol{\kappa}_{\text{eff}} \cdot \nabla_< + \frac{2Z}{r_<}\right] A(r_<) = 0 \tag{14}$$

with the solution

$$A = {}_1F_1\left(-i\frac{Z}{k_{<,\text{eff}}}, 1; -i(k_{<,\text{eff}} r_< + \boldsymbol{k}_{<,\text{eff}} \cdot \boldsymbol{r}_<)\right) \tag{15}$$

where the effective momentum for the inner electron is given by

$$\boldsymbol{k}_{<,\text{eff}} = \boldsymbol{k}_< + \nabla_< \Phi \tag{16}$$

and Φ giveb by eq. (13). This momentum modification (16) is identical to the result achieved by [18] to lowest order in $r_</r_>$. $\overline{\Psi}$ in eq. (10) has correct asymptotic behaviour also if all three particle separations are large. This is easily seen because each of the confluent hypergeometric functions reduces than to a pure phase factor, and the effective momentum (16) approaches its static value in that limit. Eq. (10) is still incorrect in the limit of two electrons close together but far away from the nucleus. We investigate therefore this limit now. To this end we introduce Jacobi coordinates $\boldsymbol{R} = \frac{1}{2}(\boldsymbol{r}_< + \boldsymbol{r}_>)$ and $\boldsymbol{r} = \boldsymbol{r}_> - \boldsymbol{r}_<$. For large values of R and finite values of r we expect of structure of the wavefunction like $\overline{\Psi} = B(\boldsymbol{r})e^{i\Lambda}$ where the phase Λ is now defined by the eikonal equation

$$\left(\boldsymbol{k}_> \cdot \nabla + \boldsymbol{k}_< \cdot \nabla\right) = \frac{Z}{r_>} + \frac{Z}{r_<} \tag{17}$$

with the solution

$$\Lambda = \frac{Z}{k_>}\ln(k_> r_> + \boldsymbol{k}_> . \boldsymbol{r}_>) + \frac{Z}{k_<}\ln(k_< r_< + \boldsymbol{k}_< . \boldsymbol{r}_<) \quad (18)$$

For the amplitude B we find the wave equation ($r << R$)

$$\left[\Delta_r + 2i\kappa_{\text{eff}} . \nabla_r - \frac{1}{r}\right] B(\boldsymbol{r}) = 0 \quad (19)$$

where κ_{eff} is given by

$$\kappa_{\text{eff}} = \frac{1}{2}(k_> - k_<) + \frac{1}{2}(\nabla_> - \nabla_<)\Lambda \quad (20)$$

We conclude therefore that the wavefunction given by eq. (10) should be an accurate solution of the Schrödinger equation provided the relative momentum κ is replaced by its effective value, see eq. (16). We intend to employ this wavefunction for future (e, $2e$) and (γ, $2e$) calculations. Although we expect the wavefunction (10) to give better results than (9) we stress that even (9) does quite well. Braauner, Briggs and Klar have demonstrated this in pilot calculations, see [?].

4. Applications of the Born approximation

The Born approximation is far behind a perfect theory, but nevertheless it provides some useful applications in the context of triply differential cross sections (TDCS). This concerns the optical limit as well as the determination of absolute TDCSs.

4.1. Optical limit :

With the wavefunction given by eq. (8) the T-matrix element for inelastic electron scattering gets the form

$$T = \frac{4\pi}{q^2}\left\langle \psi_f \left| \sum e^{i\boldsymbol{q}\cdot\boldsymbol{r}_n} \right| \varphi \right\rangle \quad (21)$$

with the momentum transfer given by $\boldsymbol{q} = \boldsymbol{k}_0 - \boldsymbol{k}_a$, the index n counts the target electrons, and φ is the initial target bound state wavefunction. Let us now consider collisions accompanied with small values of the momentum transfer. This situation can be realized with high incident energy and small angle scattering. In the extreme case of nearly zero momentum transfer we expand in eq. (21) the exponential and find

$$T = \frac{4}{q}\left\langle \psi_f \left| \hat{\boldsymbol{q}} \cdot \sum_n \boldsymbol{r}_n \right| \varphi \right\rangle \quad (22)$$

Here we have used the orthogonality $\langle \psi_f | \varphi \rangle = 0$. $\hat{\boldsymbol{q}} = \boldsymbol{q}/q$. is a unit vector along the momentum transfer direction. The above matrix elemnt (22) describes formally photoabsorption in dipole approximation, and $\hat{\boldsymbol{q}}$ plays the role of the light polarization vector. It is a well known fact that photoexcitation or photoionization may be regarded as electron scattering at zero momentum transfer. It must be stressed that the limit $q = 0$ can never really be reached in a realistic experiment. The smallest value actually occurs in forward direction. But we will see in the following that small angle scattering data are very close to photoabsorption data. Consider for instance photo-single-ionization of an s-electron in comparison to electron impact ionization of an s-electron. Since the photo-continuum- electron is a p-electron the photoelectron angular distribution is a $\cos^2\theta$ distribution, *i.e.* it looks like an *eight* axially symmetric to the electric field vector. In the electron impact ionization we also find two loops nearly axially symmetric around the momentum transfer. But the loops are different in size, and the axial symmetry is slightly broken. The departure from the optical limit is due to contributions from higher multipoles beyond the dipole.

4.2. Absolute triply differential cross sections :

The above analysis has an immediate application. Often one measures quite accurate relative TDCSs at not too large values of the momentum transfer. The angular pattern consists than of two loops, a binary loop approximately in q-direction, and a recoil peak approximately in opposite direction. Note that at finite values of q the two loops have different size. The normalization procedure may now be performed as follows. We consider several measurements at fixed incident energy but different though small momentum transfer and plot the magnitudes of the binary and recoil peaks as function of q, and extrapolate these data to $q = 0$. From 4.1 we know that the two curves must meet in one point. At this point, the optical limit, we usually know the absolute value either from another experiment or from theory. Thus we can put the relative data onto an absolute scale. Details of this method and examples for demonstration may be found in [20], see also Figure 2.

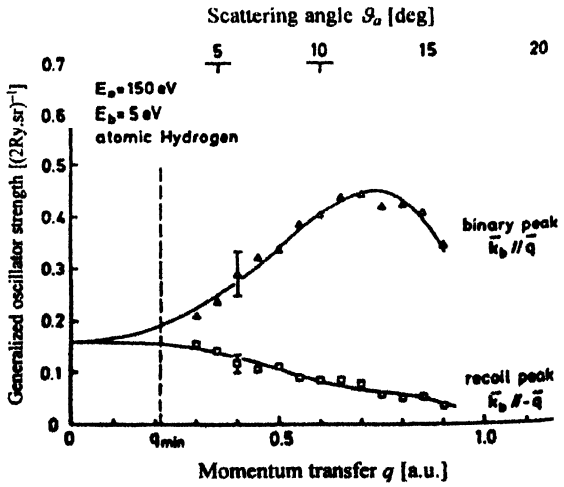

Figure 2. Generalized oscillatorstrengths of the binary peaks and the recoil peaks in the direction of the momentum transfer for 150 eV impact energy on H(1*s*). Full lines : polynomial fits to measurements for the extrapolation to the optical limit q.

Triply differential cross sections

We consider again single ionization by electron impact. In the final state we find two escaping electrons (scattered and ejected ones). Because energy conservation holds only for the whole system (ion + 2 electrons) the kinematic of the ionization process is fully determined if and only if at least the momenta of two particles (ion + 1 electron, or two electrons) are detected. Mostly one detects the electron pair in coincidence [21]. From the Born apprroximation, see 3.2, we know that we get reasonable cross sections particularly for smaller values of the momentum transfer. An overview upon the dependence on the momentum transfer is shown in Figure 3. The situation is particularly simple for initial *s*-electron. In the Born limit (close to the optical limit) we get simply two loops axially symmetric around the

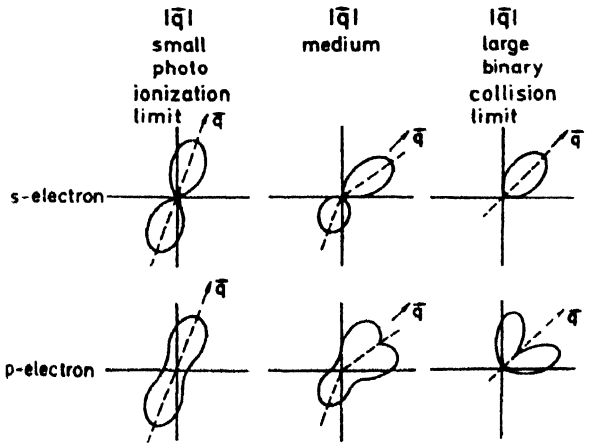

Figure 3. Triple differential cross section for the ejection of an *s*-electron (above) or a *p*-electron (below).

momentum transfer. For slightly larger q-values the axial symmetry is broken. This results from the electron-electron repulsion in the continuum. For still larger q-values the recoil loop disappears, *i.e.* we reach the binary collision limit. Experiments in the latter range are suitable to determine the initial bound state wavefunction in the momentum space [3]. Investigations at intermediate q-values are important for the study of the ionization dynamics. This article focusses on that aspect. So far we assumed that we ionize an *s*-orbital. For a *p*-orbital the situation is very similar to the preceeding one except that the binary peak may have dip, see Figure 3. This dip results from the node of the *p*-wavefunction, and appears at $k_b = q$.

The intermediate q-value range was for a long time a mystery for the theoreticians. Departures from the first Born approximation are evident, but it was unclear where they came from. Now we know that final state correlation (the electron-electron repulsion in the continuum) is the origine of it. This was first demonstrated by a second Born calculation by [24]. That treatment only indirectly and approximatively takes continuum correlation into account, but it goes into the right direction. A more direct approach was developed by Brauner, Briggs and Klar [15] who have used a final state waverfunction, see eq. (9), which has the electron-electron repulsion as an essential ingredient in it. Numerical results on that basis compare very favorably with experimental data, including the circular dichroism, see [25–27] for details, see also Figure 4. Quite generally it can be said that the BBK is most successful at not too low incident energies, but it fails to reproduce the Wannier law.

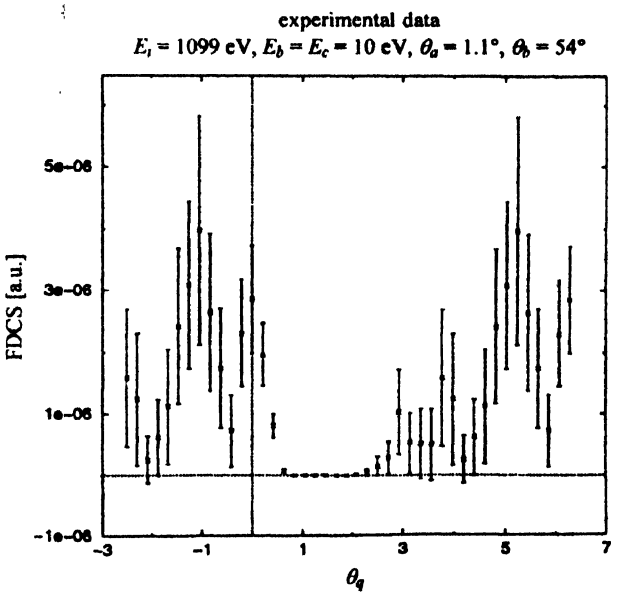

Figure 4(a). Calculated FDCS for double ionization of He. Three incident energy is E_0 = 1099 eV, the secondary electron energies are $E_b = E_c$ = 10 eV, the scattering angle is Θ_a = 1.1, one of the slow electrons is detected at 54. The plot shows the angular distribution of the other slow electron.

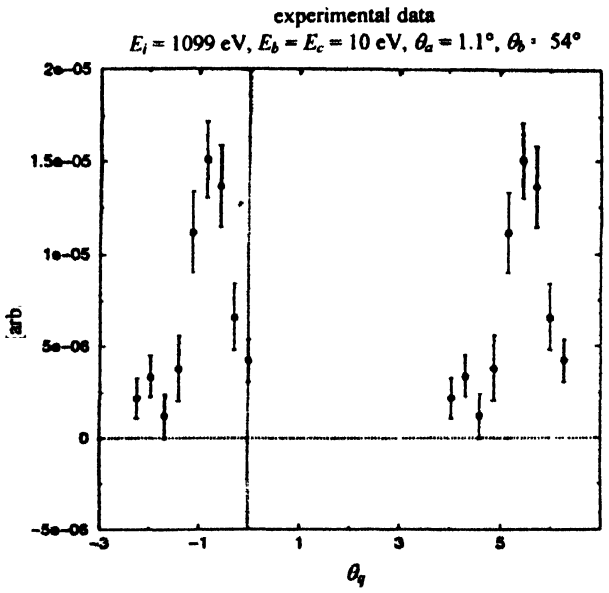

Figure 4(b). Experimental data. Kinematic as in Figure 4a.

6. Double ionization

Double ionization by electron impact with fully determined kinematics requires triple electron coincidences. These are usually refered to as $(e, 3e)$ experiment. Such experiments are since a few years possible [28]. A theory of $(e, 3e)$ runs basically along the same lines as for $(e, 2e)$. In particular a BBK-like treatment seems promizing because it takes correlation into acount. Actually it is trivial to generalize the BBK wavefunction given in eq. (9) to more than two escaping electrons. One only has to introduce more Coulomb functions in eq. (9), one per each electron-nucleus interaction and one for each electron-electron pair.

One this basis we have calculated fivefold differential cross sections, hereafter FDCS for brevity, for $(e, 3e)$ from He. Figures 4a, b show a typical examples for unequal energy sharing.

In these situations we have kept fixed the fast scattered electron and one of the secondary electrons. The angular distribution of the other secondary electron is then plotted. We remark that first Born type treatments have been tried [29]. But even at high incident energy and small momentum transfer the Born approximation leads to poor results. We believe that the main shortcoming of the Born approximation is that the two secondary electrons are automatically created in a spin singlett since the target is a singlett, namely He(^1S). Our BBK-type wavefunction properly antisymmetrized does not suffer from that.

Double ionization is often discussed in terms of a *two-step* model. Here the first step is a single ionization, this continuum electron is scattered back, collides with another target electron and ionizes that. It remains of course entirely in the dark which mechanism forces the first electron to return. In this paper we don't do such models. Our view point is that the projectile transfers energy to the target, the target is than in a high doubly excited continuum state and decays. We properly describe that decay. In our view point double collision models appear rather artificial and therefore unrealistic. So far we have completed one $(e, 3e)$ calculation on the basis of an extended BBK treatment. The incident energy is $E_0 = 1099$ eV, the target is He, the scattering angle is $\Theta = 1.1°$. The two secondary electrons have energies of $Eb = Ec = 10$ eV. One of the secondary electrons, say b, is detected at the fixed angle of $\Theta_b = 54°$, Figure 4a shows the angular distribution of the second secondary electron. The unit on the abcissa is radian measured from the momentum transfer direction (dotted line). The error bars reflect the uncertainty of the evaluation of the T-matrix element which has been performed with a Monte Carlo code. This kinematical situation has been investigated experimentally [30], see Figure 4b. Qualitatively our calculation compares well with the experiment. The incorporation of local momenta is expected to amend the results.

Acknowledgment

Financial support by SFB276 is greatfully acknowledged

References

[1] J T Tate and P T Smith *Phys. Rev.* **39** 270 (1932)

[2] W L Fite and R T Brackmann *Phys. Rev.* **112** 1142 (1958)

[3] H Bethe *Ann. Phys. (Leipzig)* **5** 325 (1930)

[4] H Ehrhardt *Zeit. Phys.* **D1** 3 (1986)

[5] M Inokuti *Rev. Mod. Phys.* **43** 297 (1971)

[6] G H Wannier *Phys Rev.* **90** 817 (1953)

[7] S Cvejanovic and F H Read *J. Phys.* **B7** 1841 (1974)

[8] H Kossmann, V Schmidt and T Andersen *Phys. Rev Lett* **60** 1266 (1988)

[9] H P Schmitt *Diplom thesis Univ. Würzburg* (1978)

[10] R Rippler, R Klar, K Saeed, I McGregor, A J Duncan and R Kleinpoppen *J. Phys.* **B16** 1617 (1983)

[11] J B Donahue, P A M Gram, M V Hynes, R W Hamm, C A Frost H C Bryant, K B Butterfield, D A Clark and W W Smith *Phys Rev. Lett.* **48** 1538 (1982)

[12] J A R Samson and G C Angel *Phys. Rev. Lett.* **61** 1584 (1988)

[13] H Klar *J. Phys.* **B14** 3255 (1981)

[14] H Klar and W Schlecht *J. Phys.* **B9** 1699 (1971)

[15] M Brauner, J S Briggs and H Klar *J. Phys.* **B22** 2265 (1989)

[16] G Garibotti and J E Miraglia *Phys. Rev.* **A21** 572 (1980)

[17] Redmond (unpublished); see L Rosenberg *Phys. Rev.* **D8** 1833 (1964)

[18] E O Alt and A M Mukhamedzhanov *Phys. Rev.* **A47** 2004 (1993)

[19] A Engelns, H Klar and A Malherek *J. Phys.* **B30** 811 (1997)

[20] K Jung, R Müller-Fiedler, P Schlemmer, H Ehrhardt and H Klar *J. Phys.* **B18** 2955 (1985)

[21] H Ehrhardt, M Schulz, T Tekaat and K Willmann *Phys. Rev Lett* **22** 89 (1969)

[22] H Ehrhardt, M Fischer, K Jung, F W Byron, C J Joachain and B Pireaux *Phys. Rev. Lett.* **48** 1807 (1982)

[23] I McCarty and E Weigold *Phys. Rep.* **27C** 27 (1976)

[24] F W Byron, C J Joachain and B Piraux *Phys. Rev. Lett.* **99A** 427 (1983)

[25] J Berakdar, A Engelns and H Klar *J. Phys.* **B29** 1109 (1995)

[26] J Viefhaus, L Avaldi, G Snell, M Wiedenhöff, R Hentges, A Rüdel, F Schäfers, D Menke, U Heinzmann, A Engelns, H Klar and U Becker *Phys. Rev. Lett.* 77 3975 (1996)

[27] A Dorn, A Elliott, J Lower, E Weigold, J Berakdar, A Engelns and H Klar *Phys. Rev. Lett.* 80 257 (1998)

[28] A Lahman-Bennani, C Dupré and A Duguet *Phys Rev. Lett.* 63 1582 (1989)

[29] C dal Capello *Priv. Comm.*

[30] A Lahman-Bennani *Priv. Comm.*